Journal of Sustainable Construction Materials and Technologies
Web page info: https://jscmt.yildiz.edu.tr
DOI: 10.29187/jscmt.2021.60

JSCMT
Journal of Sustainable Construction Materials and Technologies

Original Article

Characterization of crack healing of asphalt mixtures treated with healing agents

Martin Munene RIARA

Department of Physical Sciences, South Eastern Kenya University, Kitui, Kenya

ARTICLE INFO

Article history
Received: 8 April 2021
Accepted: 5 June 2021

Key words:
Asphalt pavements, crack healing; healing agents, healing mechanism, healing models

ABSTRACT

This study investigated the long-term crack healing of asphalt mixtures treated with healing agents (HAs). Five crack healing agents were applied on fractured surfaces of asphalt mixtures and the long-term healing performance was evaluated based on the restored peak strength and fracture energy. Long term healing of the mixtures was predicted using the Modified Wool and O'Connor model, a modified Avrami model and a long-term healing prediction model proposed in this study. Test results indicated that the proposed healing model and the modified Avrami model could predict the long-term healing of the asphalt mixtures. Crack healing comprised of an instantaneous component and a time dependent healing component. The instantaneous component was attributed to crack wetting and the adhesion of the healing agents onto the fracture surfaces. The time dependent component was ascribed to molecular flow of the HAs. Additional healing due to hardening and drying of the HAs' residue succeeded molecular flow healing. The temperature dependence of crack healing using HAs follow the Arrhenius law. The healing activation energies determined based on this law were dependent on the type of the HA. Maltene based HAs have a lower activation energy, hence, they required less energy to stimulate the recovery of the material response parameters.

Cite this article as: Riara MM. Characterization of crack healing of asphalt mixtures treated with healing agents. J Sustain Const Mater Technol 2021;6:2:53–62.

INTRODUCTION

Asphalt binder is a self-healing material i.e., after the loading stresses are withdrawn, it can spontaneously recover partially or totally to its original operational health and functionality [1, 2]. This self-healing ability is limited for modified asphalt binders and their composites with fillers and graded aggregates. [3]. In order to improve the healing ability of asphalt mixtures, researchers have identified techniques such as infusion of microcapsules/microfibers containing rejuvenators into construction mixtures [4-6], induction heating of mixtures reinforced with metallic additives [7-13] and surface treatments using healing agents [6, 14, 15].

There is general consensus that healing play a role, and perhaps a significant role in the performance and service

***Corresponding author.**
*E-mail address: mriara@seku.ac.ke

This paper was recommended for publication in revised form by Regional Editor Benchaa Benabed.

life of asphalt pavements. Actually, research points out that if an asphalt pavement is allowed enough rest time, crack-based damage could be spontaneously repaired to some extent [16-18]. Nevertheless, when the crack-based damage is beyond the threshold for macro cracking, self-healing alone is ineffective in reversing the structural health of the pavement. Self-healing and extrinsically induced crack healing are complex processes dependent on several factors such as: temperature, binder aging, extent of cracking, duration of rest periods and so on. The underlying healing mechanisms and the governing processes are not well understood. Direct measurements and/or observation of the actual healing mechanism is challenging and unfeasible. Therefore, predictive models have been proposed to reveal the healing process and enable the characterization of the constituent governing processes [19-22].

Different theories which include: molecular diffusion healing model, capillary flow healing model, phase field healing model and the surface energy healing model have been proposed to explicate the intrinsic fracture healing process. These theories were developed depending on the choice of the fundamental parameter, type and conditions of the test method as well as the healing index (HI) adopted. The molecular diffusion healing model is based on interfacial healing as proposed by Wool and O'Conner [22]. According to this theory, intrinsic healing occurs in three successive steps: (1) wetting of the crack surfaces; (2) instantaneous gain in strength due to interfacial cohesion; and (3) long term gain in strength caused by inter-diffusion and randomization of the molecules across the cracked surfaces. Wool and O'Conner determined that a macroscopic healing function, R, was the result of convolution of the wetting distribution function, ϕ(t), and the intrinsic healing function, Rh(t), over a time variable, τ, according to Eq. 1.

$$R = \int_{-\infty}^{t} R_h(t-\tau)\frac{d\phi}{d\tau}d\tau \quad (1)$$

The initial healing process (wetting stage) involves crack surface wetting which is determined by the crack closure speed, □, around the healing process zone, β according to Eq. 2 [23].

$$\frac{d\phi\,(tX)}{dt} = \dot{a} = \beta\left[\frac{1}{D_1 K_m}\left\{\frac{\pi W_c}{4(1-\nu^2)\sigma_h^2\beta}D_o\right\}\right]^{1/m} \quad (2)$$

Where Wc is work of cohesion, and υ is Poisson's ratio. Do, D1 and m are creep compliance parameters determined by fitting D(t)=D_o+D_1 t^m and Km is a material constant determined from m. Further, the terminal two stages which are mainly due to the molecular diffusion across the damage sites were defined according to Eq. 3. This molecular flow healing occur due to a complex simultaneous processes of diffusion [24-28], capillarity [29], reptation [30, 31] and randomization [32, 33] of the molecules within the neighborhood of the treated crack interface.

$$R_h = R_o + Kt^{0.25}.\,\xi(t) \quad (3)$$

Rh is the net macroscopic healing due to wetting and molecular flow. Ro and K are the instantaneous healing and time dependent healing terms respectively. ξ(t) represents the effect of surface rearrangement with time during the healing process.

Molecular flow healing would be determined accurately only if the molecular structure of the flowing material is known. However, establishing the molecular structure of asphalt binders or healing agents is certainly not feasible. Therefore, different models have been used to predict the molecular flow healing process. Based on the thermodynamics of healing, Sun et al proposed that the short-term macroscopic healing determined from a predefined healing index (HI) could be related to the instantaneous and short term strength gain according to Eq. 4 [34].

$$HI\,(T,t) = HI_0 + Kt^n \quad (4)$$

HI is a function of healing temperature, T and time, t and HIo denotes the instantaneous HI. K is the temperature dependent healing ratio due to diffusion and capillarity which proceed at a rate denoted by n. The value of n ranges from 0.25-0.5 for asphalt materials. Using a different approach, Bommavaram and Little proposed that the net macroscopic healing could be modelled using a modified form of the Avrami equation given by Eq. 5 [19].

$$R_h = R_o + p(1 - e^{-qt^r}) \quad (5)$$

Where Ro and $(1 - e^{-qt^r})$ represent the instantaneous healing caused by interfacial work of cohesion or surface free energy and time dependent healing resulting from molecular inter-diffusion respectively. p, q, and r are independent material constants. These constants are postulated to relate to material properties such as activation energy, molecular weight, temperature and pressure, though, the correlation is not well understood.

In this study, five crack healing agents were used to heal fractured semicircular samples of AC-13 asphalt mixtures. The short- and long-term healing performance of the mixtures was determined based on the recovered peak strength and fracture energy as determined according to AASHTO TP105 [35]. The main objectives of this paper was to (a) propose an appropriate model to predict the long term crack healing of asphalt mixtures treated with healing agents, (b) describe the molecular flow healing term in terms of its rates of healing with time and temperature, (c) provide a limited validation of the proposed model, (d) establish the temperature dependence of the healing process and (e) calculate the HAs' activation energies.

MATERIALS AND EXPERIMENTAL TECHNIQUES

Materials

Basalt aggregates and limestone filler were used to prepare AC-13 basalt asphalt mixtures. Figure 1 and Table 1 shows the aggregate gradation and properties of the aggregates and filler respectively. SBS modified asphalt with a penetration value of 73dmm, viscosity of 0.645Pa.s at 135 °C, ductility

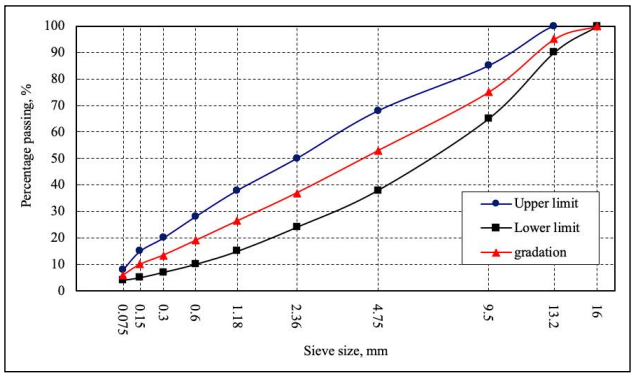

Figure 1. Gradation of the AC-13 asphalt mixtures.

Table 1. Properties of basalt aggregates and Limestone filler

Basalt aggregate	**%**
Crushed stone value	12
Los Angeles abrasion value	7.8
Flakiness & elongation index	8.5
Specific gravity (g/cm^3)	2.96
Limestone filler	**%**
Density (g/cm^3)	2.83
Chemical composition	
CaO	51.8
SiO_2	3.49
Al_2O_3	1.29

of 52.1 at 5 °C and softening point of 68 °C was used as the binder. The optimum content of the binder was determined as 4.7% using Marshall design method with specimens compacted with 75 blows per face. Base bitumen emulsion (BBE), Styrene-butadiene rubber modified bitumen emulsion (SBRE) and three maltene based commercial pavement maintenance cationic emulsions (HA-1, HA-2, and HA-3) were used as healing agents in this study. BBE and SBRE are standard emulsions used in chip seals, micro-surfacing and flush coats. HA-1, HA-2, and HA-3 have a high content of aromatics which is reported to be crucial for self-healing of asphalt materials [36-38]. The chemical composition and viscosity of the emulsions and their residues is shown in Table 2.

Sample Preparation and Testing

A Superpave gyratory compactor (Troxler-4140, USA) was used to compact the mixtures to Ndesign of 75 gyrations. The compacted mixtures were then cored to 100mm diameter cylinders. Later, semi-circular bending (SCB) samples with a thickness of 25mm, diameter of 100mm and a notch length of 10mm were then prepared according to AASHTO TP-105 [35]. Before testing, the SCB samples were preconditioned at -10 °C for 4 hours to create a brittle fracture and to avoid creep deformation [9, 11, 39]. SCB testing was conducted using a universal testing machine (UTM-25, Australia) using a monotonic loading rate of 0.5mm/min until total failure (strength of 0 kPa). After the test, the specimens were allowed to equilibrate to room temperature (25 °C). For each test, three replicates were prepared and tested. This approach maintained the data within a standard deviation of at most 5%. Any data that had a standard deviation of 10% or more (of the mean of the other two data points) was considered an outlier and for such cases, additional tests were conducted to correct the anomaly.

A soft brush was used to apply the HAs on the fractured surfaces at a rate ranging from 0.4–0.7 kg/m^2, to avoid excessive bleeding of the agents. An effective residue content of about 0.25–0.35 kg/m^2 remained on the treated cracks after drying of the HAs. The difference in effective residue content was reasonably small and its influence on healing was considered to be insignificant. The samples were then carefully placed together and stored in a direction normal to the cracked surface so that the weight of the upper half of the sample would squeeze out any excessive HA. The samples were in 9 groups which were tested after healing at 25 °C for 1, 2, 4, 8, 15, 30, 60, 90 and 120 days. In order to validate the healing model and calculate the healing activation energies of the HAs, additional mortar and mixture samples were prepared and tested after healing for 1, 2, 4, 8, 15, 30 and 60 days at 35 and 45 °C. Mortar was designed to correspond to the mortar phase in the mixtures. The optimum content of the binder in mortar was determined as 9.2% using the fine fraction in the asphalt mixture.

Table 2. Viscosity and chemical composition of healing agents

Healing Agent	**Chemical composition (%)**				**Viscosity**	
	Saturates	**Aromatics**	**Resins**	**Asphaltenes**	**Residue at 60 °C (Pa.s)**	**Emulsion at 25 °C (cP)**
HA-1	22.1	58.9	10.4	8.6	15-20	160-180
HA-2	18.1	48.6	22.2	11.1	140-160	50-70
HA-3	12.2	70.1	11.2	6.5	100-120	45-65
BBE	14.1	29.6	43.5	12.8	210-230	150-170
SBRE	13.4	25.8	49.3	11.5	700-900	40-60

Crack healing was assessed based on the recovery of peak strength and fracture energy. Our earlier study revealed that these material response properties give a more precise and accurate impression of healing [40]. The healing indexes determined from peak strength (PI) and fracture energy (EI) were defined according to Eqs. 6 and 7 respectively.

$$PI = \frac{F_h}{F_i} \times 100 \quad (6)$$

$$EI = \frac{E_h}{E_i} \times 100 \quad (7)$$

$$E_{h\ or\ i} = \frac{\sum_i^n \frac{1}{2}(F_{i+1}+F_i)(d_{i+1}-d_i)}{(r-a)t} \quad (8)$$

Where F and E are the peak strength and fracture energy respectively. The subscripts 'i' and 'h' designate the initial value and the value measured after healing respectively. di is the displacement at the ith position when the loading force is Fi while a, r and t are the specimen's crack length, radius and thickness respectively.

RESULTS AND DISCUSSIONS

Models for healing assessment

Figure 2 (a-f) show the healing curves of the mixtures treated with different HAs. Figure 2 (a, b) show the curves modelled using the modified Wool and O'Connor model (Eq. 4) while Figure 2 (c, d) show the curves modelled using the modified form of Avrami model (Eq.5). The fit parameters for both models are summarized in Table 3.

Poor fitting with relatively low coefficient of determination values (R^2) indicated that Eq. 4 was inappropriate for prediction of long-term healing of asphalt mixtures treated with healing agents. From the curves in Figure 2 (a, b), it is clear that the model could predict short term healing of the mixtures but it failed when the healing duration was longer than 30 days. This model predicted that crack healing was a continuously increasing phenomenon which could induce peak strength and fracture energy higher than the initial values when the healing duration was sufficiently long. However, the experimental data indicated that there existed an optimum healing time when crack healing reached a maximum value which was lower than the initial measured value.

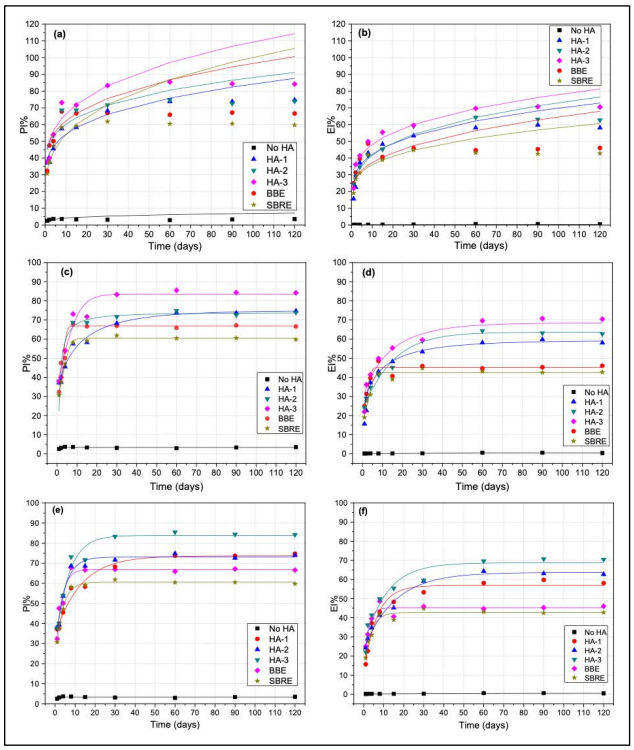

Figure 2. Crack healing of asphalt mixtures modelled using Eq. 4 **(a, b)**, Eq. 5 **(c, d)** and Eq. 9 **(e, f)**.

Figure 2 (c, d) and table 3 shows that Eq. 5 had good fitting and relatively high R^2 with an average global fit accuracy of 97.6%. This implied that it was a better model for

Table 3. Summary of the fit results.

HA	HI	Eq. 4 fit parameters				Eq. 5 fit parameters					Eq. 9 fit parameters			
		HIo (%)	K (%)	n	R_2	R_o (%)	P (%)	q	r	R_2	A (%)	B (%)	to (days)	R_2
No HA	PI	0.12	2.41	0.23	0.50	2.41	0.94	0.13	3.5	0.99	4.06	3.34	0.62	0.94
	EI	0.01	0.10	0.18	0.63	0.18	0.36	1.93	3.58	0.90	0.57	0.44	40.7	1.00
HA-1	PI	22.9	16.2	0.29	0.79	26.8	48.3	0.21	0.67	0.97	73.7	51.5	6.84	0.97
	EI	12.3	15.8	0.28	0.89	15.7	43.7	0.27	0.6	0.99	57.7	40.6	8.38	0.98
HA-2	PI	24.7	20.0	0.25	0.81	31.3	34.1	0.22	1.04	0.99	73.1	46.9	4.50	0.97
	EI	6.80	18.4	0.28	0.98	24.1	39.5	0.05	1.08	0.99	63.7	40.0	15.4	0.98
HA-3	PI	24.7	20.6	0.31	0.81	37.8	45.7	0.06	1.34	0.94	83.8	55.3	6.52	0.96
	EI	16.0	16.8	0.28	0.93	27.5	41.0	0.11	0.85	0.99	70.7	43.9	11.1	0.93
BBE	PI	31.2	14.9	0.32	0.57	30.9	35.9	0.04	2.52	0.99	67.0	47.7	2.94	0.94
	EI	17.8	8.20	0.38	0.60	23.9	21.3	0.06	2.37	0.99	46.0	23.2	10.5	0.92
SBRE	PI	28.1	19.4	0.33	0.73	30.7	29.8	0.06	1.81	0.99	60.6	40.5	3.47	0.99
	EI	16.7	11.3	0.30	0.64	19.1	23.3	0.06	2.05	0.99	42.7	26.3	9.72	0.94

prediction of both short- and long-term healing of the mixtures. The model indicated that there was an instantaneous gain in material properties denoted by Ro and a time dependent component equal to P. Component P increased with increase in healing time in a complex exponential manner governed by the model parameters q and r as defined by Eq. 5. According to this model, the mixtures treated with HAs had 26–38% and 15–38% of the initial peak strength and fracture energy respectively restored instantaneously. A further 30–49% and 21–44% of initial peak strength and fracture energy respectively was recovered as a time dependent component. Though this model fitted the experimental data well, it introduced two independent constants q and r that were not well defined. Their inter-correlation or relationship with other physical properties of the mixtures is unknown. In addition, these constants did not show a consistent trend, and hence, they could not be relied upon to explain the time dependent healing of the mixtures. For these reasons, a simpler empirical model was proposed to predict the short- and long-term healing of the mixtures. Eq. 9 was proposed to model the long-term healing of the mixtures.

$$HI\ (T,t) = A(T) - B(T)exp\left[\frac{-(t-\tau)}{t_o}\right] \quad (9)$$

A(T), B(T), τ and to represents the ultimate HI, molecular flow HI, HAs' volatilization time and the shift point respectively. Below to the gain in HI is rapid and beyond it, the gain tends to be steady. The proposed model has two fundamental terms related to the instantaneous healing and the ultimate healing. These terms are defined by Eqs. 10 and 11 respectively.

$$Ultimate\ healing = \lim_{t\to\infty} HI(T,t) = \lim_{t\to\infty}\left\{A(T) - B(T)exp\left[\frac{-(t-\tau)}{t_o}\right]\right\} = A \quad (10)$$

$$Time\ dependent\ healing\ factor = \lim_{t\to\infty} HI(T,t) - \lim_{t\to\tau} HI(T,t) = B \quad (11)$$

In this model, the HA's volatilization time, τ was considered to be much shorter than the healing time, t (i.e., t >> τ). The trends in each of the fundamental terms were used to identify the time dependent healing rate in each of the stages. It is important to note that just like Eq. 5, Eq. 9 predicts that crack healing of the mixtures using healing agents comprises of an instantaneous component (equal to A-B) and a time dependent component (equal to B). This equation was considered to be a better model because in addition to good fitting and high R^2 values (average global fit accuracy of 96.0%), its parameter to indicated a physical parameter which is the transition time when healing shifts from initial to intermediate stage. The fit parameters for the model are also summarized in Table 3.

Figures 2 (c–f) show that healing of treated mixtures occurred in 3 stages. They include the initial (0~4 days), intermediate (4~60 days), and the tertiary (60~120 days) healing stages. The initial and intermediate stages are time dependent molecular flow due to diffusion, capillarity, reptation and randomization of the HAs. The molecular flow was rapid in the initial stage, slower in the intermediate stage and nearly static in the tertiary stage. Rapid healing during the early age healing is expected because immediately after contact, there is fast molecular flow (diffusion, capillarity and reptation) of the HAs into the crack surfaces. The decline in the rate of healing in the intermediate stage could be the result of decreased rates of diffusion and capillarity. There was minimal healing at the tertiary stage when a concentration equilibrium was attained and the flow processes ceased. The transition time to for peak strength and fracture energy ranged from 3.5–7 days and 8–11.5 days respectively. The optimum healing time t_{max} defined as the time required for the recovered material properties to reach a plateau was determined as 15-30 days and 30–60 days for peak strength and fracture energy respectively. Therefore, based on to and t_{max}, the recovery of peak strength preceded the restoration of fracture energy regardless of the choice of the HA.

There is an instantaneous, though limited recovery of material properties for the wetted crack portion due to interfacial work of adhesion between the HAs and the cracked surfaces. This work of adhesion is a function of the surface free energy. The measured value of the work of adhesion at the time of wetting is minimal. However, the true contribution of the wetting process is realized after the evaporation/volatilization of the emulsified HAs into residues. The evaporation/ volatilization process occur simultaneously with the molecular flow (diffusion, capillarity and reptation) of the HAs. In fact, the flow processes are rapid before evaporation/volatilization of the HAs. Therefore, it is difficult to isolate the contribution of the both processes from the healing value determined as the instantaneous component. Therefore, the analysis in this paper focused on the rates of healing at each stage and not the contribution of each of the constituent processes proposed by Wool and O'Connor. To elucidate the healing mechanism, the healing stages were further analyzed to reveal the characteristic governing processes. As mentioned earlier, the choice of the model defined by Eq. 9 seems reasonable based on the good fitting and high R^2 values presented in Table 3.

Molecular Flow Healing Stage

Molecular flow healing comprises of healing resulting from both the wetting by the HAs and the diffusion, capillarity and reptation of the HAs into the neighborhood of the crack surfaces. Crack wetting occur when the polar low molecular weight HA fragments weld together with similar dangling chain ends created during scission of the binding scale in the course of cracking. Meanwhile, the long molecular fragments remain entangled within the matrix of the HAs. The macroscopic consequence of the welding process is an instantaneous gain in material properties after the volatilization of water in the HAs. The wetting rate depends on both the surface free energy of the HAs and the strength of the chemical forces such as van der Waals forces or electrostatic dipole polarity of the agents and the crack surface. Cationic emulsions adhere to the crack surfaces due to the

polar attraction of Lewis acids and bases. Such HAs have a high affinity for electrons while the anionic basalt mixtures are rich in electrons. Therefore, acid base interactions at the crack surface result in wetting due to the 'breaking' of the HAs. In addition to the electrostatic acid-base interactions, the abundance of the low molecular weight aromatic fractions in maltene based HAs could also be responsible for the adhesion induced by the HAs. The overall effect of the acid base interactions and the welding phenomena manifests as an intimate HA-crack surface interfacial adhesion that restores a fraction of the material properties. Nevertheless, it would be difficult to quantify and characterize the contribution of each based on the macroscopic healing.

The adhesion of the HAs residue onto the crack surfaces is followed by a time and temperature dependent healing process. In order to establish the variation of the processes governing this stage, the molecular flow factor B(T) was determined for the initial, intermediate and tertiary stages and the results are shown in Figure 3.

The molecular flow rate decreased gradually from the initial to the tertiary healing stage. Unlike maltene based HAs, traditional bitumen emulsions show a high molecular flow rate in the initial healing stage but this rate decay rapidly in the successive stages due to their rapid drying rate. Generally, the molecular flow healing stage constitutes an initial rapid gain in material properties, followed by a slower intermediate healing stage, and lastly, a nearly static tertiary stage. In these stages, molecular flow of the HAs led to softening and reconstitution of the aged binder's chemical and physical properties. The flux of the molecules continues to erase the concentration gradient between the HAs and the aged binder until a concentration equilibrium is attained. Beyond this equilibrium, self-diffusion via reptation could also occur albeit to a very limited extent.

The gradual gain of material properties in the initial healing stage is postulated to be due to the entanglement of the molecular chains, and the repair of intermolecular secondary bonds and other forces linking the microstructures

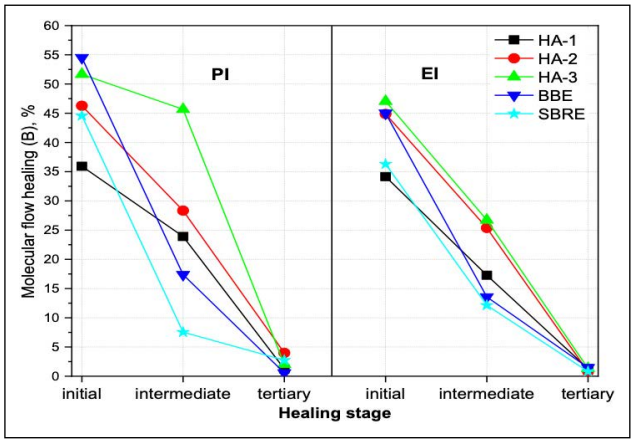

Figure 3. Molecular flow healing rate at initial, intermediate and tertiary stages.

in the reconstituted binder. This phenomenon restores mainly the stiffness modulus of the cracked region. In the intermediate healing stage, viscosity of the HAs' residue begins to increase due to the loss of volatile components via evaporation and volatilization. The formation of chemical bonds and the solidification of the HAs residue create a strongly bound 'solid wedge' between the crack surfaces. The solidified wedge retards further crack growth and also act as a mechanical force transmission bridge at the interface which improve the crack's load bearing and transfer capability. As mentioned earlier, the restoration of stiffness modulus and strength, precede the recovery of the dissipated and surface free energies which are attributed to the formation of the force transmitting solid wedge. The healing mechanism and the characteristic processes are illustrated in Figure 4 and 5.

Tertiary Healing Stage

This is the terminal healing stage where molecular flow processes are expected to have ceased. It is characterized by a small gain in fracture energy and negligible gain in strength. The gain in fracture energy could be attributed to the continued hardening of the HA's residue which recovers the ability of the healed region to resist crack initiation, opening and further propagation. The ultimate healing determined in this stage is the sum of bridging effect due with the adhesion of the HA on the crack flanks, and the cohesion due to crack closure effect associated with the rigid solid wedge formed by the HAs' residue.

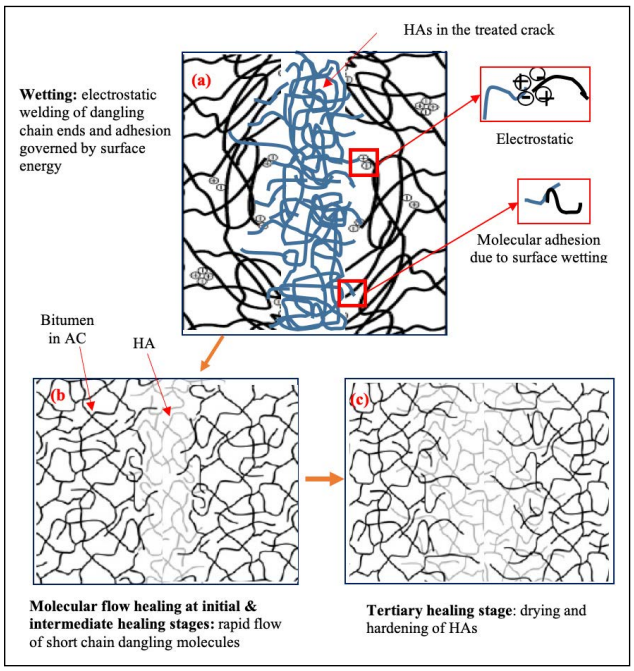

Figure 4. Schematic of chain movement during healing of fractured interface using HAs, wetting effect **(a)** molecular flow healing at initial and intermediate stages **(b)**, tertiary stage **(c)**.

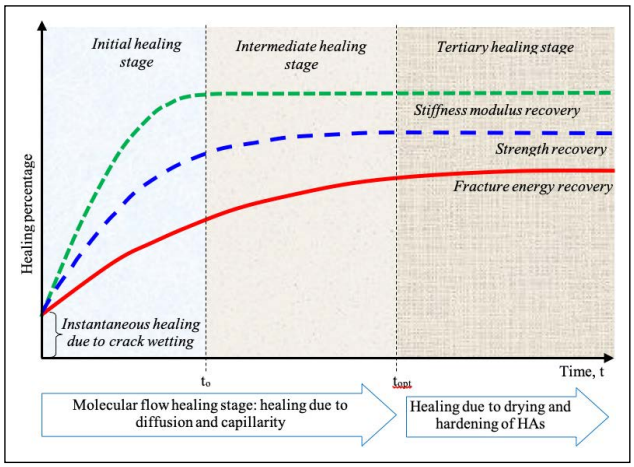

Figure 5. Conceptual illustration of crack healing using HAs.

Temperature Dependence of the Healing Process

Crack healing is a temperature dependent process. Increase in temperature improves the instantaneous healing by lowering the surface free energy of both the HAs and the aged binder in the asphalt pavement. Similarly, the rates of diffusion and capillarity hasten at elevated temperatures due to the increased molecular mobility and penetration depth. Therefore the temperature dependence of the healing process could be modelled using temperature dependence flow models such as the Arrhenius equation defined by Eq. 12 [21].

$$B(T) = B_o \exp\left(\frac{-E_h}{RT}\right) \quad (12)$$

Where Bo, T and R are the molecular flow constant, absolute temperature and universal gas constant (8.314 J/mol/K) respectively. Eh is the healing activation energy which signifies the minimum energy for flow (via diffusion, capillarity and reptation) and randomization of the HA molecules into the crack surfaces. Eq. 12 could be incorporated in the proposed healing model Eq. 9 to yield Eq. 13 which is a universal short- and long-term healing prediction model.

$$HI\ (T,t) = A(T) - \left[B_o \exp\left(\frac{-E_h}{RT}\right)\right] exp\left[\frac{-(t-\tau)}{t_o}\right] \quad (13)$$

The macroscopic molecular flow dependent healing ratio, B(T), of asphalt mixtures determined at 25, 35 and 45oC was modelled using the Arrhenius Eq. 12 and the fit results are presented in Figure 6 (a, b). An additional fit for intrinsically healed asphalt mortar is included in the figure for the purpose of validating the model.

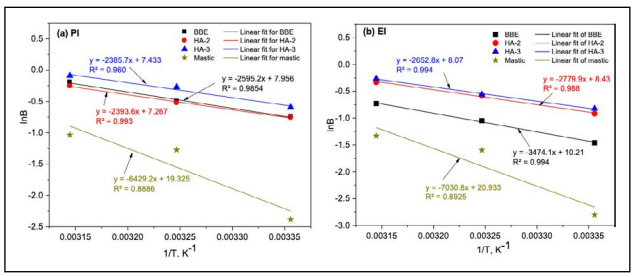

Figure 6. Macroscopic molecular flow healing of asphalt mortar and mixtures modelled using Eq. 12.

The fit results and the high R^2 values presented in Figure 6 (a, b) indicate that the molecular flow healing of mixtures treated using HAs follow the Arrhenius model Eq. 12. This confirms that healing of asphalt materials using HAs is a temperature dependent process. The fit also indicate that there exists a threshold energy required for the healing process to be stimulated. Henceforth, an energy equal or greater than Eh must be supplied to the damaged site for the time dependent healing to be initiated. For that reason, a HA with a low activation energy would be favorable because the lower the healing activation energy barrier, the less the energy needed for the healing process to be triggered. Linear regression was used to determine the healing activation energy of the HAs based on the fit results determined from Figure 6 (a, b). Figure 7 presents the healing activation energy for the HAs.

The healing activation energy for asphalt mastic determined using PI and EI was 53.5kJ/mol and 58.5kJ/mol respectively. These results are very close to the Eh of 50.97kJ/mol determined for short term healing of the same mastic by Sun et al [21] using a mesoscale healing evaluation approach and the modified Wool and O'Connor molecular diffusion healing model (Eq. 4) [22]. Therefore, the proposed universal healing evaluation model Eq. 13 is suitable for characterization of long-term healing performance of asphalt materials treated with HAs. It is clear from figure 7 that Eh of BBE is higher than that of maltene based HAs. Eh determined using PI cannot distinguish HA-2 and HA-3 but based on Eh determined from EI, HA-3 has a lower healing activation energy. These results also confirm that HA-3 is a better macro-crack HA for asphalt materials.

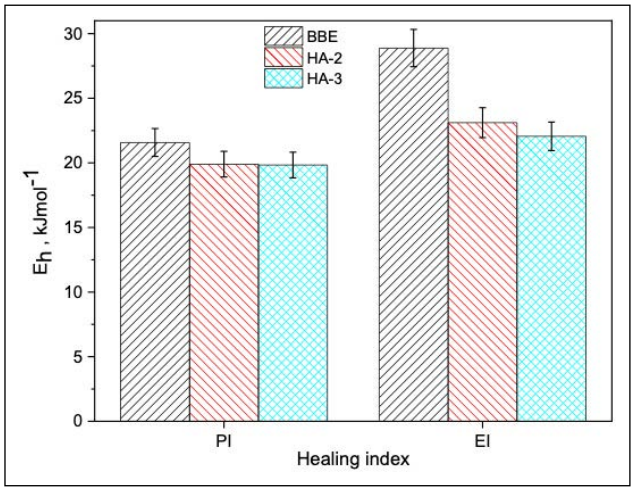

Figure 7. Activation energy, Eh, of different HAs.

CONCLUSIONS

Fractured SCB samples of AC-13 basalt asphalt mixtures were healed using five macro-crack HAs. Test samples were healed for 1 to 120 days and the recovered peak strength and fracture energy were used to evaluate their healing. The long-time healing data was first modelled using modified Wool and O'Connor model and modified Avrami model. Later, a four-stage healing model was built to fit the long-time healing results of asphalt materials. The proposed model was used to assess the characteristic healing mechanism(s) during the different healing stages. The following conclusions were drawn from the test results and analysis done.

i). The proposed long-time crack healing prediction model and the modified Avrami model could predict the long-term healing of asphalt mixtures using healing agents. The proposed model was more suitable because it was less complex and all its model parameters have a physical meaning.

ii). Macro-cracks of asphalt mixtures healed in three stages: the initial (0~4 days); intermediate (4~60 days) and tertiary (60~120 days) healing stages. The time dependent molecular flow was rapid in the initial stage, slower in the intermediate stage and nearly static in the tertiary stage.

iii). Macroscopic healing could be described using the molecular flow healing model. Adhesion of the HAs residue onto the crack surfaces was due to surface wetting by the action of electrostatic and acid-base interactions. During the molecular flow healing stage, diffusion, capillarity and reptation of the HA molecules enabled the softening and reconstitution of the aged binder. Further healing resulted from drying and hardening of the HA's residue which act as a mechanical stress transmitting bridge to retard further crack growth and improve the crack's load bearing and transfer capability.

iv). The temperature dependence of crack healing using HAs follow the Arrhenius law. The healing activation energies determined based on this law were dependent on the type of the HA. Maltene based HAs have a lower activation energy, hence, they require less energy to stimulate the recovery of the material response parameters.

Conflict of Interest:

The authors declare that they have no conflict of interest.

Financial Disclosure:

The authors declared that this study has received no financial support.

Peer-review:

Externally peer-reviewed.

REFERENCES

[1] Bekas, D.G., Tsirka, K., Baltzis, D., Paipetis, A.S. (2016). Self-healing materials: A review of advances in materials, evaluation, characterization and monitoring techniques. Composites Part B: Engineering, 87, 92-119. https://doi.org/10.1016/j.compositesb.2015.09.057.

[2] Gupta, S., Pang, S.D., Kua, H.W. (2017). Autonomous healing in concrete by bio-based healing agents – A review. Construction and Building Materials, 146, 419-428. https://doi.org/10.1016/j.conbuildmat.2017.04.111.

[3] Liang, B., Lan, F., Shi, K., Qian, G., Liu, Z., Zheng, J. (2021). Review on the self-healing of asphalt materials: Mechanism, affecting factors, assessments and improvements. Construction and Building Materials, 266, 120453. https://doi.org/10.1016/j.conbuildmat.2020.120453.

[4] Shen, J., Amirkhanian, S., Aune Miller, J. (2007). Effects of Rejuvenating Agents on Superpave Mixtures Containing Reclaimed Asphalt Pavement. Journal of Materials in Civil Engineering, 19(5), 376-384. https://doi.org/10.1061/(ASCE)0899-1561(2007)19:5(376).

[5] Rushing, J.F., Falls, A.J., Field performance of asphalt surface treatments on airfields, International Conference on Pavement Preservation, 1st ed, California Department of Transportation, Federal Highway Administration Foundation for Pavement Preservation, California, USA, 2010. https://www.pavementpreservation.org/icpp/paper/48_2010.pdf

[6] Riara, M., Tang, P., Mo, L., Javilla, B., Wu, S. (2018). Investigation into crack healing of asphalt mixtures using healing agents. Construction and Building Materials, 161, 45-52. https://doi.org/10.1016/j.conbuildmat.2017.11.074.

[7] Liu, Q., Schlangen, E., García, Á., van de Ven, M. (2010). Induction heating of electrically conductive porous asphalt concrete. Construction and Building Materials, 24(7), 1207-1213. https://doi.org/10.1016/j.conbuildmat.2009.12.019.

[8] Dai, Q., Wang, Z., Mohd Hasan, M.R. (2013). Investigation of induction healing effects on electrically conductive asphalt mastic and asphalt concrete beams through fracture-healing tests. Construction and Building Materials, 49, 729-737. https://doi.org/10.1016/j.conbuildmat.2013.08.089.

[9] Apostolidis, P., Liu, X., Scarpas, A., Kasbergen, C., van de Ven, M. (2016). Advanced evaluation of asphalt mortar for induction healing purposes. Construction and Building Materials, 126, 9-25. https://doi.org/10.1016/j.conbuildmat.2016.09.011.

[10] García, A., Bueno, M., Norambuena-Contreras, J., Partl, M.N. (2013). Induction healing of dense asphalt concrete. Construction and Building Materials, 49, 1-7. https://doi.org/10.1016/j.conbuildmat.2013.07.105.

[11] Norambuena-Contreras, J., Garcia, A. (2016).

Self-healing of asphalt mixture by microwave and induction heating. Materials & Design, 106, 404-414. https://doi.org/10.1016/j.matdes.2016.05.095.

[12] Apostolidis, P., Liu, X., Kasbergen, C., Scarpas, A.T., van de Ven, M. (2017). Toward the Design of an Induction Heating System for Asphalt Pavements with the Finite Element Method. Transportation Research Record, (2633), 136-146. https://doi.org/10.3141/2633-16.

[13] Pamulapati, Y., Elseifi, M.A., Cooper, S.B., Mohammad, L.N., Elbagalati, O. (2017). Evaluation of self-healing of asphalt concrete through induction heating and metallic fibers. Construction and Building Materials, 146, 66-75. https://doi.org/10.1016/j.conbuildmat.2017.04.064.

[14] Lin, J., Hong, J., Huang, C., Liu, J., Wu, S. (2014). Effectiveness of rejuvenator seal materials on performance of asphalt pavement. Construction and Building Materials, 55, 63-68. https://doi.org/10.1016/j.conbuildmat.2014.01.018.

[15] Riara, M., Tang, P., Mo, L., Hong, W., Chen, M., Wu, S. (2018). Evaluation of moisture and temperature effect on crack healing of asphalt mortar and mixtures using healing agents. Construction and Building Materials, 177, 388-394. https://doi.org/10.1016/j.conbuildmat.2018.05.020.

[16] Tan, Y., Shan, L., Richard Kim, Y., Underwood, B.S. (2012). Healing characteristics of asphalt binder. Construction and Building Materials, 27(1), 570-577. https://doi.org/10.1016/j.conbuildmat.2011.07.006.

[17] Qiu, J., van de Ven, M., Wu, S., Yu, J., Molenaar, A. (2011). Evaluating Self Healing Capability of Bituminous Mastics. Experimental Mechanics, 52(8), 1163-1171. https://doi.org/10.1007/s11340-011-9573-1.

[18] Castro, M., Sánchez José, A. (2006). Fatigue and Healing of Asphalt Mixtures: Discriminate Analysis of Fatigue Curves. Journal of Transportation Engineering, 132(2), 168-174. https://doi.org/10.1061/(ASCE)0733-947X(2006)132:2(168).

[19] Bommavaram, R., Bhasin, A., Little, D. (2009). Determining Intrinsic Healing Properties of Asphalt Binders. Transportation Research Record: Journal of the Transportation Research Board, 2126, 47-54. https://doi.org/10.3141/2126-06.

[20] Riara, M., Tang, P., Mo, L., Chen, M., Zhang, J., Wu, S. (2018). Experimental assessment of the long-time crack healing in asphalt mixtures using healing agents. Construction and Building Materials, 191, 411-422. https://doi.org/10.1016/j.conbuildmat.2018.10.001.

[21] Sun, D., Lin, T., Zhu, X., Cao, L. (2015). Calculation and evaluation of activation energy as a self-healing indication of asphalt mastic. Construction and Building Materials, 95, 431-436. https://doi.org/10.1016/j.conbuildmat.2015.07.126.

[22] Wool, R.P., O'Connor, K.M. (1981). A theory crack healing in polymers. Journal of Applied Physics, 52(10), 5953-5963. https://doi.org/10.1063/1.328526.

[23] Schapery, R.A. (1989). On the mechanics of crack closing and bonding in linear viscoelastic media. International Journal of Fracture, 39(1), 163-189. https://doi.org/10.1007/bf00047448. https://doi.org/10.1007/BF00047448.

[24] Ma, T., Huang, X., Zhao, Y., Zhang, Y. (2015). Evaluation of the diffusion and distribution of the rejuvenator for hot asphalt recycling. Construction and Building Materials, 98, 530-536. https://doi.org/10.1016/j.conbuildmat.2015.08.135.

[25] Cong, P., Hao, H., Zhang, Y., Luo, W., Yao, D. (2016). Investigation of diffusion of rejuvenator in aged asphalt. International Journal of Pavement Research and Technology, 9(4), 280-288. https://doi.org/10.1016/j.ijprt.2016.08.001.

[26] Xiao, Y., Li, C., Wan, M., Zhou, X., Wang, Y., Wu, S. (2017). Study of the Diffusion of Rejuvenators and Its Effect on Aged Bitumen Binder. Applied Sciences, 7(4), 397. https://doi.org/10.3390/app7040397.

[27] Xu, H., Zhou, J., Dong, Q., Tan, Y. (2017). Characterization of moisture vapor diffusion in fine aggregate mixtures using Fickian and non-Fickian models. Materials & Design, 124, 108-120. https://doi.org/10.1016/j.matdes.2017.03.076.

[28] Bhasin, A., Little, D.N., Bommavaram, R., Vasconcelos, K. (2011). A Framework to Quantify the Effect of Healing in Bituminous Materials using Material Properties. Road Materials and Pavement Design, 9(sup1), 219-242. https://doi.org/10.1080/14680629.2008.9690167.

[29] García, Á. (2012). Self-healing of open cracks in asphalt mastic. Fuel, 93, 264-272. https://doi.org/10.1016/j.fuel.2011.09.009.

[30] Wu, D.Y., Meure, S., Solomon, D. (2008). Self-healing polymeric materials: A review of recent developments. Progress in Polymer Science, 33(5), 479-522. https://doi.org/10.1016/j.progpolymsci.2008.02.001.

[31] Gennes, P.G.d. (1971). Reptation of a Polymer Chain in the Presence of Fixed Obstacles. The Journal of Chemical Physics, 55(2), 572-579. https://doi.org/10.1063/1.1675789.

[32] Garcia, S.J. (2014). Effect of polymer architecture on the intrinsic self-healing character of polymers. European Polymer Journal, 53, 118-125. https://doi.org/10.1016/j.eurpolymj.2014.01.026.

[33] Sun, D., Sun, G., Zhu, X., Guarin, A., Li, B., Dai, Z., et al. (2018). A comprehensive review on self-heal-

ing of asphalt materials: Mechanism, model, characterization and enhancement. Advances in Colloid and Interface Science, 256, 65-93. https://doi.org/10.1016/j.cis.2018.05.003.

[34] Sun, D., Sun, G., Zhu, X., Pang, Q., Yu, F., Lin, T. (2017). Identification of wetting and molecular diffusion stages during self-healing process of asphalt binder via fluorescence microscope. Construction and Building Materials, 132, 230-239. https://doi.org/10.1016/j.conbuildmat.2016.11.137.

[35] American Association of State Highway and Transportation Officials, AASHTO TP 105: Standard method of test for determining the fracture energy of asphalt mixtures using the Semicircular Bend geometry (SCB), AASHTO, Washington DC, USA, 2013.

[36] Sun, D., Yu, F., Li, L., Lin, T., Zhu, X.Y. (2017). Effect of chemical composition and structure of asphalt binders on self-healing. Construction and Building Materials, 133, 495-501. https://doi.org/10.1016/j.conbuildmat.2016.12.082.

[37] Little, D.N., Lytton, R.L., Williams, D., Kim, R. (1998). An Analysis of the Mechanism of Microdamage Healing Based on the Application of Micromechanics First Principles of Fracture and Healing. Journal of Association of Asphalt Paving Technologists, 68, 501-542. http://worldcat.org/issn/02702932.

[38] Schmets, A., Kringos, N., Pauli, T., Redelius, P., Scarpas, T. (2010). On the existence of wax-induced phase separation in bitumen. International Journal of Pavement Engineering, 11(6), 555-563. https://doi.org/10.1080/10298436.2010.488730.

[39] Al-Qadi, I.L., Fini, E.H., Figueroa, H.D., Masson, J., McGhee, K.K., Adhesion testing procedure for hot-poured crack sealants, 2008. https://rosap.ntl.bts.gov/view/dot/16703.

[40] Riara, M., Tang, P., Mo, L., Javilla, B., Chen, M., Wu, S. (2018). Systematic Evaluation of Fracture-Based Healing Indexes of Asphalt Mixtures. Journal of Materials in Civil Engineering, 30(10), 04018264. https://doi.org/10.1061/(ASCE)MT.1943-5533.0002479.